



## FOUR SWITCH THREE PHASE FREQUENCY CONVERTER USING LINEAR-QUADRATIC REGULATOR CONTROLLER

V.Harshini<sup>1</sup>, N.Raja rajeswari<sup>2</sup>, Sd.Munvar Basha<sup>3</sup>, K.Hemalatha<sup>4</sup>,

P.V.Chaitanya<sup>5</sup>, M.Ajay<sup>6</sup>, L.Mastanamma

<sup>1,2,3,4,5,6</sup>Under graduate in Department of EEE

<sup>7</sup>Assistant Professor in Department of EEE

<sup>1,2,3,4,5,6,7</sup> QIS College Of Engineering and Technology

### ABSTRACT

This research study examines the efficiency of a wind power conversion system that utilizes a four-button three-phase converter. The converter is powered by a generator, and the control technique is determined by the Linear-Quadratic Regulatory authority Controller. The VS-Wind Generator 8Generator Solution (WTGS) utilizes a permanent-magnet synchronous generator (PMSG) to drive the variable-speed system. This system is connected to the grid by a regularity converter that has full capacity. A dc-link connects both power converters that make up the frequency converter. Furthermore, this analysis presents a comparison of the system performance between four-button inverters and six-switch inverters, specifically in terms of the pace of response and harmonic distortion of stator currents. This study considers realistic wind rate values in order to get valuable and significant responses. The

LQR controller is used to evaluate the performance of the system by comparing the results. The Linear-Quadratic Regulator (LQR) is a recommended alternative controller that aims to provide long-lasting control stability and optimal dynamic performance, while avoiding complex control schemes. The MATLAB/Simulink environment is often used in simulation studies that employ proportional-integral controllers based on the Grey Wolf algorithm. To demonstrate the effectiveness of the LQR controller in enhancing the efficiency of the WTGS. To further validate the results, the simulated outputs are compared to the experimental results. to enhance system security and effectively manage system volatility.

### I.INTRODUCTION

This research proposes an optimal control strategy to maximize the efficiency of a wind energy conversion system (WECS). The linear-quadratic regulator (LQR)



formula, known for its rapid convergence and little mathematical complexity, is considered the optimal control strategy. The LQR controller is used to modify both the device and grid-side converter/inverter. The system design and its corresponding control techniques are shown. In order to get accurate replies, this research considers real wind speed data. The system's efficiency is examined by comparing the results generated by the LQR controller with those produced by using maximized proportional-integral controllers based on the grey wolf optimizer algorithm, while taking into account significant network disruptions. The effectiveness of the LQR controller in enhancing the performance of the WECS is shown via extensive simulations carried out using the MATLAB/Simulink environment. To enhance validation, the simulation results are compared to the conjectural information.

The stator currents are generated due to harmonic distortion via the use of a four-button and six-switch inverter. This experiment allows us to see and confirm the existence of results, while confirming the rate of elimination at various levels. By implementing a three-stage four-switch inverter with a lower number of switches, the cost of the inverter is reduced. The six-switch configuration is used to detect faults such as open or short circuits in the inverter. By using symmetrical and crucial controllers in the superconducting technology, we may develop a magnetic energy storage system. The voltage source inverter relies on the cascaded symmetrical indispensable control technique. The use of flock optimization is necessary in order to

achieve proportionate integral. The term "proportional indispensable" refers to both the actual and reactive abilities. The magnetic power-based proportional integral controller is developed using the swarm optimization approach. The Consistency Search Algorithm (CSA) is used to prioritize the importance of proportional factors. The software may be constructed using MATLAB, and the simulation results have been verified. The voltage source inverter may reduce the variability of regularity. This document illustrates the configuration of the Proportional-Integral-Derivative (PID) controller in the AVR system using the Transcriptional Cancer Genome Atlas (TCGA). The strategy may compare and differentiate between the genetic algorithm technique and the flock optimization method. The Proportional-Integral-Derivative (PID) controller is a crucial component of the Automatic Voltage Regulator (AVR) system.

Photovoltaic (PV) installations are seeing steady worldwide expansion, resulting in a significant integration into the electric grid. The DC-DC converter is implemented to maintain a constant voltage in the DC microgrid. The GWO formula has a resemblance to the organizational structure and hunting strategy of grey wolves in the natural world. Our findings suggest that wolf-pack hunting is a kind of collective behaviour that does not depend on visible communication among the individuals involved in the hunt.

This study applies a new approach by using a grey wolf optimizer (GWO) to enhance the ability of a grid-connected permanent-



magnet synchronous generator powered by a variable-speed wind generator (DD-PMSG-VSWT) to handle decreased voltage events (LVRT) and optimize power factor tracking (MPPT). The LVRT capabilities and MPPT enhancements are accomplished by the precise adjustment of eight proportional-integral (PI) controllers in the cascade policy of the grid-side inverter and machine-side converter. An online optimization technique is used to minimize the integral-squared error of the input errors of PI controllers that regulate the DC link voltage, generated real power, and terminal voltages of the Permanent Magnet Synchronous Generator (PMSG) and the power grid. This proposes an optimum control method aimed at achieving maximum efficiency of a wind power conversion system (WECS). The choice of the best control strategy relies on the linear-quadratic regulator (LQR) formula, which offers rapid convergence and reduced mathematical complexity. The LQR controller is used to readjust the machine and the grid-side converter/inverter. This research study presents the system design and its control methodologies. Functional The research incorporates wind rate data to ensure the accuracy of the activities shown. The performance of the structure is assessed by comparing the results obtained using a LQR controller with those achieved when optimized proportional-integral controllers based on the grey wolf optimizer algorithm are used, taking into consideration significant network disruptions. The simulation research investigations are conducted meticulously using the MATLAB/Simulink environment to validate the effectiveness of the LQR

controller in enhancing the performance of WECS. The simulation findings are being compared to experimental data in order to further enhance recognition. Systems equipped with classic LQR controllers exhibit significant stability features and are well-suited for a certain performance criterion.

## II. MODEL OF THE WIND TURBINE

Mathematical expression for the output power extracted from the wind is represented as

$$P_{\omega} = 0.5\rho\pi R^2 V_{\omega}^3 C_p(\lambda, \beta)$$

..... (1)

$P_{\omega}$  = Output power from the wind

$\rho$  = Density of air [kg/m<sup>3</sup>]

$R$  = Radius of the turbine's blade [m]

$V_{\omega}$  = Wind speed [m/s]

$C_p$  = Power coefficient

$\lambda$  = Tip speed ratio

$\beta$  = Blade pitch angle [deg.]

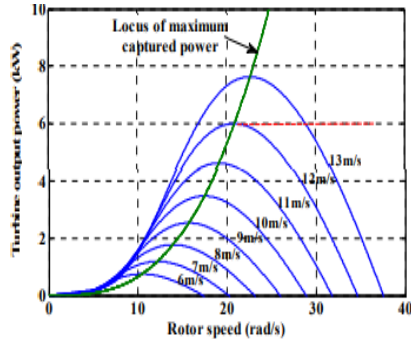


Fig. 1. Wind turbine characteristics with MPPT.

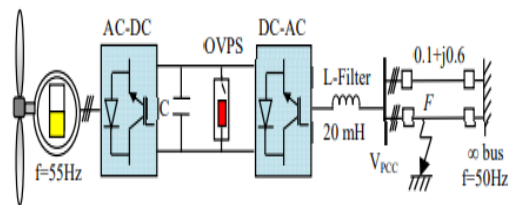


Fig. 2. Model system.

The  $C_p$  coefficient is

$$C_p(\lambda, \beta) = 0.5(\lambda - 0.022\beta^2 - 5.6)e^{-0.17\lambda} \dots\dots\dots (2)$$

$$\lambda = \frac{\omega_r R}{V_w} \dots\dots\dots (3)$$

Where,  $\omega_r$ =Blade rotor speed [rad/s].

Fig.1 shows the characteristics of the wind turbine with the maximum powerpoint tracking (MPPT).

The maximum output power from the wind in terms of rotor is as mentioned below

$$P_{max} = 0.5\rho\pi R^2 \left(\frac{\omega_r R}{\lambda_{opt}}\right)^3 C_{p-opt} \dots\dots\dots (4)$$

$C_{p-opt}$  =Optimum value of the  $C_p$ .

$\lambda_{opt}$  =Optimum value of  $\lambda$ .

### III. MODEL SYSTEM

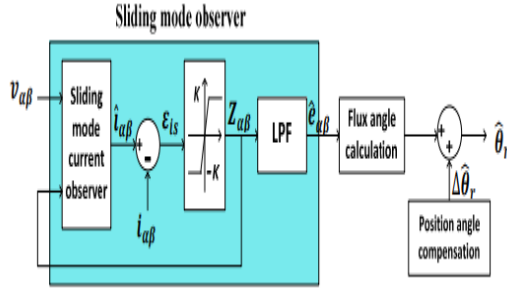
Figure 2 illustrates the system modelling utilized to describe the effectiveness of the proposed Linear Quadratic Regulator (LQR) control in regulating the frequency converter of a Variable-Speed Wind Turbine (VSWT) driving a Permanent Magnet Synchronous Generator (PMSG). The VSWT-PMSG system comprises a dual-circuit transmission line, a fully capable frequency converter, and a VSWT that are interconnected with an electrical network.

Given the following information: Rated power = 6.0 KW PMSG's frequency = 55 Hz

### IV.Speed Estimator Utilizing SMO Methodology

Understanding the precise details of the rotor position signal of the PMSG is crucial for effectively managing the system. This examination considers the use of the sliding-mode observer (SMO) to estimate the rotor position of the permanent magnet synchronous generator (PMSG) without using a sensor. The estimation is based on the recorded stator voltages and currents. The input voltages and currents of the SMO are represented using  $\alpha\beta$  coordinates in this scenario.

The  $\alpha\beta$  stator current is composed of the following components:



SYHEMATIC DIAGRAM OF THE ROTOR POSITION ESTIMATION USING PMO

$$\frac{di_{\alpha}}{dt} = -\frac{R_s}{L_s} i_{\alpha} + \frac{1}{L_s} v_{\alpha} - \frac{i}{L_s} e_{\alpha}$$

$$\frac{di_{\beta}}{dt} = -\frac{R_s}{L_s} e_{\beta} + \frac{1}{L_s} v_{\beta} - \frac{i}{L_s} e_{\beta}$$

$$e_{\alpha} = -w_{e\lambda_m} \sin\theta_r$$

$$e_{\beta} = w_{e\lambda_m} \cos\theta_r$$

Where  $R_s$  = Stator Resistance of the PMSG

$L_s$  = Synchronous inductance of the PMSG

$(v_{\alpha}, v_{\beta})$  =  $\alpha\beta$  quantities of the stator voltages

$(i_{\alpha}, i_{\beta})$  =  $\alpha\beta$  quantities of the stator currents

$(e_{\alpha}, e_{\beta})$  =  $\alpha\beta$  quantities of the stator back EMFs

$\theta_r$  = Rotor orientation

The following is an expression for the SMO technique's stator current components.

$$\frac{d\hat{i}_{\alpha}}{dt} = -\frac{R_s}{L_s} \hat{i}_{\alpha} + \frac{1}{L_s} v_{\alpha} - \frac{i}{L_s} e_{\alpha}$$

$$\frac{d\hat{i}_{\alpha} \hat{E}}{dt} = -\frac{R_s}{L_s} \hat{i}_{\beta} + \frac{1}{L_s} v_{\beta} - \frac{1}{L_s} e_{\beta}$$

$$Z_{\alpha\beta} = ksgn\epsilon_{is} = ksgn(i_{\alpha\beta} - \hat{i}_{\alpha\beta}) \frac{di_{\beta}}{dt}$$

Denotes estimated quantities

$\wedge$  = Switching Signal

$()$  = Sign Function

$\theta_r$  = switching gain of the observer

Where K selected such as  $e_{is} \cdot \left(\frac{d}{dt} \epsilon_{is}\right) < 0$

A low pass filter is estimated as back emf utilized to obtain to estimated back EMF as the  $Z_{\alpha\beta}$  as following equation

$$\hat{E}_{\alpha} = \frac{\omega_c}{s + \omega_c} Z_{\alpha}$$

$$\hat{E}_{\beta} = \frac{\omega_c}{s + \omega_c} Z_{\beta}$$

$\omega_c$  = cut off frequency

It estimated rotor position can be obtained as

$$\hat{\theta}_r = -\tan^{-1} \left( \frac{\hat{E}_{\alpha}}{\hat{E}_{\beta}} \right)$$



For filter causes delay we needed estimate angle and it is obtained as

$$\hat{\theta}_r = -\tan^{-1} \left( \frac{\omega_e}{\omega_c} \right)$$

Hence estimated rotor speed can be obtained using the derivative of the estimated rotor angle

### V. FREQUENCY CONVERTER MODELING AND CONTROL STRATEGY:

The VSWT-PMSG regularity converter, as shown in Figure 4, comprises two identical FSTP power converters. One converter is used for the converter function, while the other is used for the inverter function. Additionally, there is a two-split capacitor in the dc-link A.

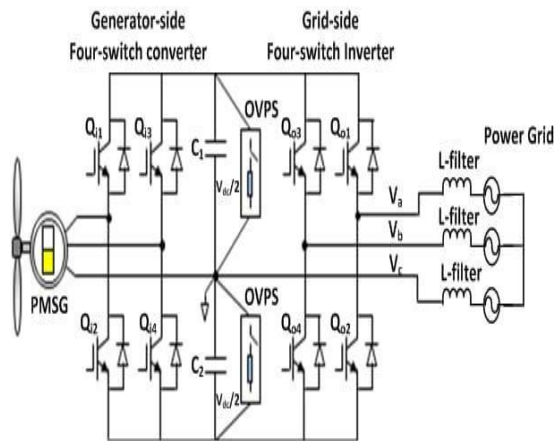


Fig: Electrical configuration of VSWT-PMSG

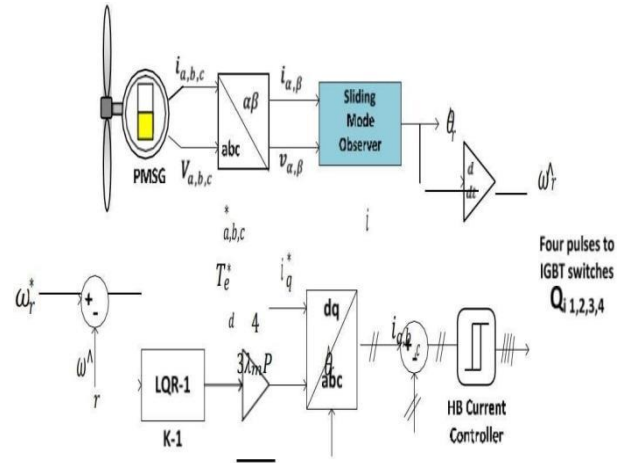


Fig: Control blocks for the MSC

The FSTP inverter, equipped with a two-split capacitor, achieves a balanced three-phase output to the electrical grid, providing adjustable voltage and frequency. The terminals of the generator are directly connected to both the pulse width modulation voltages of the converter and the central point of the two-split capacitor. The output of the two-leg inverter is connected to the three-phase electrical grid and the same central point. The split-capacitor's omphalos functions as the third stage for the converter/inverter. The GSI The main purpose of the GSI is to ensure a harmonious power element functioning inside the grid and to regulate and maintain the dc-link voltage (Vdc) at the desired value. For this experiment, two dc-link capacitors with a capacitance of 500 μF are being considered. The voltage chosen for each capacitor is 700 V. The hysteresis-based



controller is used to monitor the dc-link reference voltage and manage the GSI. The LQR controller is used to create the current along the x-axis by comparing the error signal between the reference and actual dc-link voltages. They have control over their active power. Both independent hysteresis comparators provide the triggering pulses that are sent to the two-leg rectifier.

## VI. THE SUMMARY CONTROLLER

### LQR CONTROLLER

The LQR is an optimal controller that enhances the system response by choosing an appropriate state-feedback gain matrix and using a state-space system representation.

The optimal post position in LQR is determined based on the cost function. The system use differential equations to depict the trajectories of the control variables in order to minimize the price attribute.

Although the calculation of matrix values may be readily done using this approach, the LQR is a preferable option for systems with higher order and many inputs, since it provides the

optimal feedback for the closed loop system. The determination of the optimal pole locations in LQR is dependent on the cost function. It employs differential components to reduce the cost characteristic. The exceptional service, which decreases the cost per unit area ( $J$ ), is achieved by the use of the control input.

$$J = \int_0^{\infty} (x_e^T Q x_e + u_c^T R u_c) dt$$

Here Q and R represents the Weighted-matrices,

which are chosen to create the posts at the required location. The closed-loop poles ( $E = A - BK$ ) shift towards the left side of the complex plane when the matrix has large values. As a result, the error rapidly approaches zero. The matrices, denoted as  $Q$  and  $R$ , are selected to be both positive definite and positive definite, respectively, in order to produce the desired matrix. The following is the outcome of the control input chosen to minimize the square cost function:

$$u_c = -Kx_e$$

Here,  $x_e = x_{ref} - x_{actual}$



The outlet the algebraic equation is solved, resulting in the realization of the ideal control scheme:

$$A^T P + PA - PBR^{-1}B^T P + Q = 0$$

As a result, the ideal k is found to be:

$$K = R^{-1}B^T P$$

The control system is linearized in the state-space form throughout this operation in the following manner:

$$X = AX + BU$$

$$Y = CX$$

Here  $X$  refers to the state variables,  $U$  represents the control input, and  $Y$  represents the control output. For the PMSG model, the  $X$ ,  $U$ , and  $Y$  can be represented as follows:

$$X = [i_{d-PMSG} i_{q-PMSG} \omega_e]^T$$

$$U = [V_{ds-PMSG} V_{qs-PMSG} \lambda_m]^T$$

$$Y = [i_{d-PMSG} i_{q-PMSG} \omega_e]^T$$

The  $X$ ,  $U$ , and  $Y$  for the power grid model are expressed as follows:

$$X = [i_{d-Grid} i_{q-Grid}]^T$$

$$U = [V_{ds-Grid} V_{qs-Grid}]^T$$

$$Y = [i_{d-Grid} i_{q-Grid}]^T$$

Where  $V_{ds-Grid}$  and  $V_{qs-Grid}$  show the network voltages for the X-axes.

The performance index  $J$  in this study is shown by the error signal between the set-point and real signals. The LQR controller's input is the error signal.

## OPTIMIZED PI CONTROLLER BY GWO ALGORITHM

GWO is a recently developed population-based technique introduced in 2014. The GWO formula delineates the hunting methods used by grey wolves. Grey wolves once exhibited gregarious behaviour by living in packs. Each pack often consists of 5-12 wolves. This team is often categorized into four main dominating types, known as alpha ( $\alpha$ ), beta ( $\beta$ ), delta ( $\delta$ ), and omega ( $\omega$ ) wolves. The wolves symbolize the dominant wolves of the pack. They are responsible for managing social and activity-related tasks, such as organizing hunts, determining sleep locations, and setting wake-up times. In addition, the wolves engage in intra-team predation as a means of establishing a kind of democratic hierarchy. The wolves have a higher position within the pack hierarchy, providing support and maintaining the wolves' decision-making process. The wolf is the optimal contender to assume the role of alpha when the current alpha dies or becomes too elderly. The wolves are responsible for assisting their fellow wolves and advancing the team's hierarchical structure. The wolves, which are the last ones to be allowed to eat, symbolize the team's highest degree of power. Occasionally, the wolves fulfill the role of the group's caregivers. The wolves are responsible for providing extensive information to the wolves, but they also govern them. Grey wolf searching therapies may be categorized into the following groups: The user's text is a range from 16 to 18, inclusive. 1. Monitoring, pursuing, and approaching the objective.





2. Ambush the target and relentlessly follow it until it surrenders.

3. Initiate an assault on the target. This research utilizes the GWO approach to determine the values of the PI controllers.

## VII.RESULTSANDDISCUSSION:

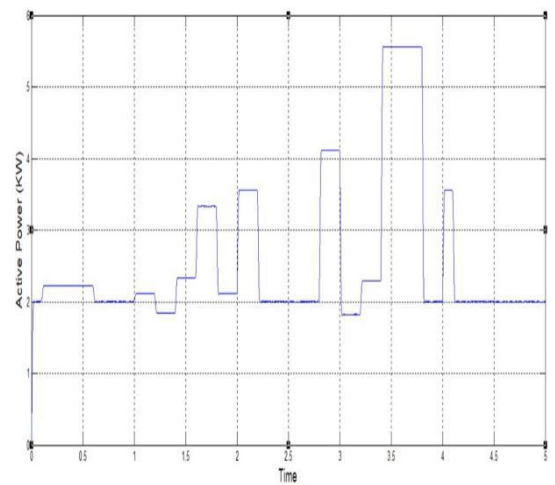
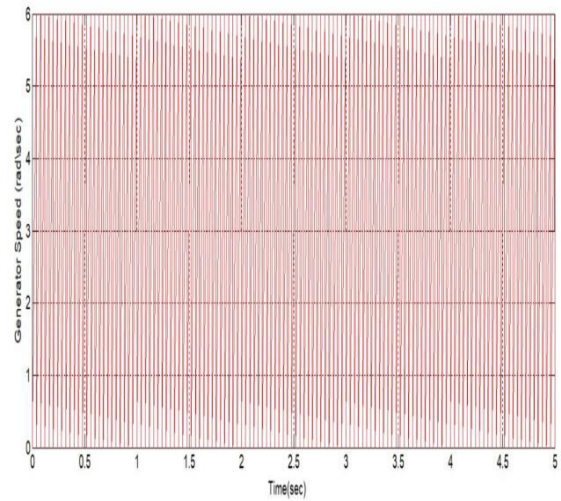
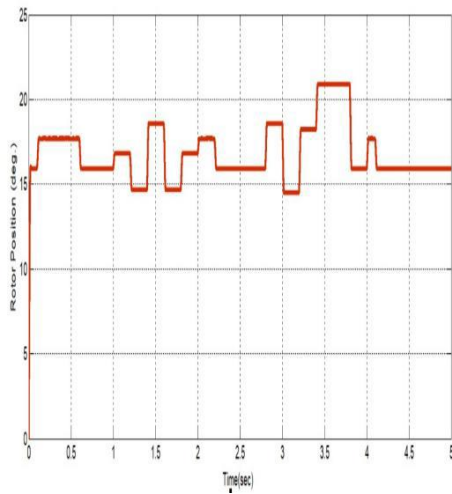
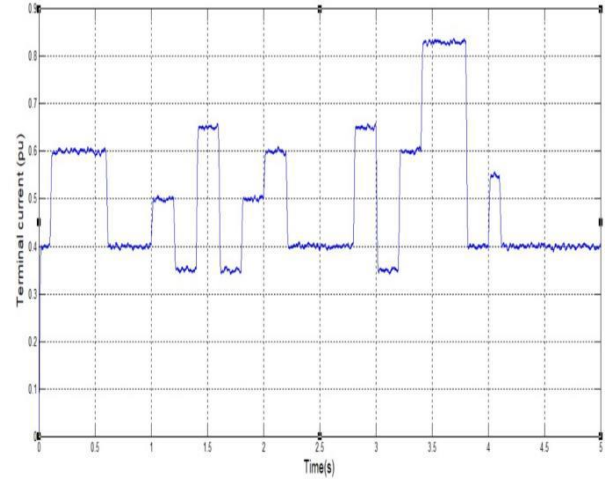
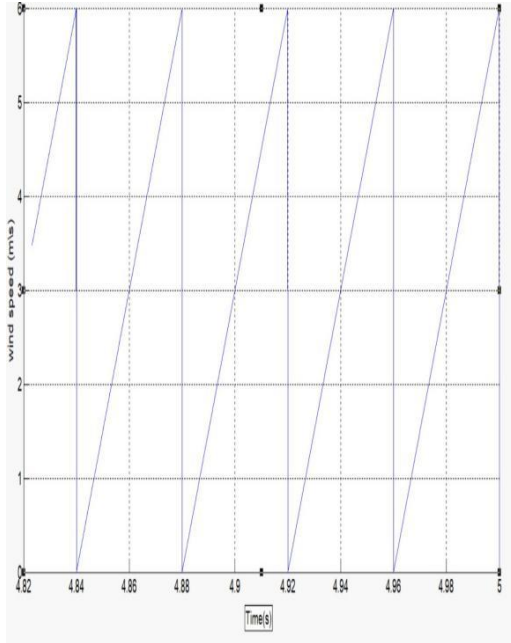
### Normal Operating Condition

The time step is 20 microseconds. The efficiency of the LQR controller is evaluated by comparing the analyses with those obtained when using the GWO. The applied controllers are based on maximal PID principles, taking into consideration both steady-state and dynamic operation conditions, which are described below. A. The simulation time of 500 seconds encompasses a broad spectrum of wind speeds, ranging from 8.1 to 11.8 meters per second. The research study illustrates the impact on the projected and measured generator rates. Below, it is evident that the calculated PMSG speed nearly corresponds to the expected speed.

The FSTP frequency converter is very compatible with the VSWT-PMSG system. Under addition, the LQR controller can accurately measure and transmit the highest amount of wind power to the energy grid under different operational scenarios.

### Transient Fault Operating Condition

The effectiveness of the LQR controller in regulating the power converters of the VSWT-PMSG integrated into the network is confirmed by exposing the system to severe grid disturbances. The three-line-to-ground (3LG) fault occurs precisely at 1.5 seconds at the fault location F, as shown. The circuit breakers (CBs) of this transmission line are simultaneously opened at 1.6 seconds in order to clear the problem. The fault is cleared after 1.7 seconds, and the circuit breakers are closed simultaneously at 2.5 seconds. The wind speed stays steady at 12 m/s. During a fault scenario, an overvoltage protection strategy (OVPS), described in [28], is used in this inquiry. The Vdc's answers with or without applying OVPS. The LQR controller outperforms the maximized PI controller based on the GWO algorithm when it comes to addressing the incurable grid voltage reaction at the PCC. The GSI's ability to respond effectively is shown by the use of both strategies.

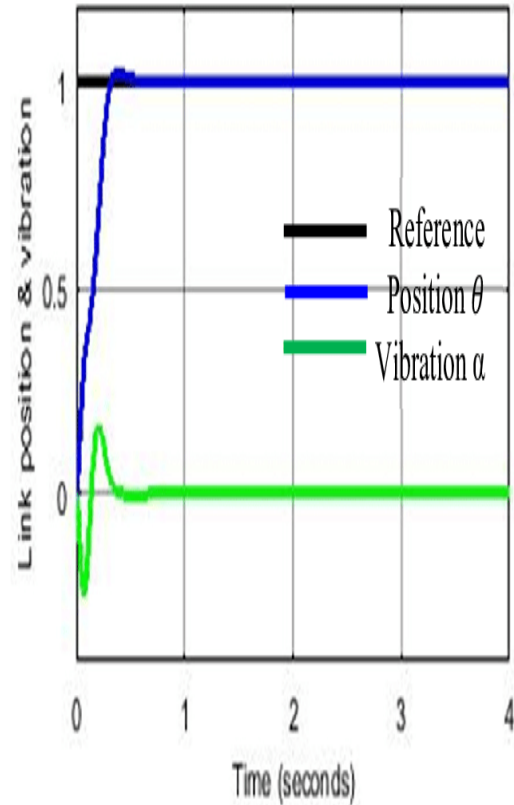




## VIII. EXPERIMENTAL RESULTS

The optimum control approach is dependent on the use of linear-quadratic regulatory authority (LQR). The arrangement consists of two sets of irreversible magnet synchronous equipment that are coupled together. The original invention functions as an electric motor to replicate the outcome of a wind turbine. The second functions as a power generator. A permanent magnet synchronous motor (PMSM) is formed by the interaction of two magnetic fields, one on the stator and one on the rotor.

### Experimental Setup of PMSM Drive



## IX. CONCLUSION

In conclusion, the ruling provides guidance for using a LQR control technique to effectively regulate the FTSP regularity converter, hence enhancing the residential characteristics of the WECS. The proposed control mechanism was designed to regulate the operations of the generator side inverter (GSI) and the device side converter (MSC).

The position of the rotor and the speed of the Permanent Magnet Synchronous Generator (PMSG) have been calculated using the Side Mode Observer (SMO) technique. The cost and integrity will undoubtedly be improved by eliminating



the blades' position and speed detecting components and using fewer power switches. The effectiveness of the LQR controller in achieving optimal responses has been validated by simulation and experimental findings, as shown by a comparison with the GWO algorithm-based optimized PI control approach. The LQR controller consistently satisfies transient criteria such as ideal percentage overshoot, undershoot, risetime, resolving time, and A number of variables, resulting in significantly reduced steady state errors compared to the PI controller. This results in a reduced memory capacity, ease of implementation, and simplicity for the LQR controller. The findings have also shown the seamless and dynamic functioning of the system, using actual wind speed data obtained from a wind power facility. Consequently, it can be inferred that the LQR is the optimal control technique as it adeptly manages the unpredictability of the system while simultaneously enhancing system stability.

## REFERENCES

- [1] Global Wind Energy Council (GWEC), "Annual market update 2015," Global Wind Report, available at: <http://www.gwec.net>
- [2] X. Zeng, J. Yao, Z. Chen, W. Hu, Z. Chen, and T. Zhou, "Co-ordinated control strategy for hybrid wind farms with PMSG and FSIG under unbalanced grid voltage condition," *IEEE Trans. Sustain. Energy*, vol. 7, no. 3, pp. 1100–1110, 2016.
- [3] Mahmoud A. Soliman, Hany M. Hasanien, Haitham Z. Azazi, et al., "Hybrid ANFIS-GA-based control scheme for performance enhancement of a grid-connected wind generator," *IET Renew. Power Gener.*, vol. 12, no. 7, pp. 832–843, 2018.
- [4] Z. Zhang, F. Wang, J. Wang, J. Rodríguez, and R. Kennel, "Nonlinear direct control for three-level NPC back-to-back converter PMSG wind turbine systems: experimental assessment with FPGA," *IEEE Trans. Ind. Inf.*, vol. 13, no. 3, pp. 1172–1183, 2017.
- [5] J. Chen, T. Lin, C. Wen, and Y. Song, "Design of a unified power controller for variable-speed fixed-pitch wind energy conversion system," *IEEE Trans. Ind. Electron.*, vol. 63, no. 8, pp. 4899–4908, 2016.
- [6] Mahmoud A. Soliman, Hany M. Hasanien, Haitham Z. Azazi, et al., "An adaptive fuzzy logic control strategy for performance enhancement of a grid-connected PMSG-based wind turbine," *IEEE Trans. Ind. Inf.*, vol. 15, no. 6, pp. 3163–3173, June 2019.
- [7] M. K. Metwally and H. Z. Azazi, "Four-switch three-phase inverter performance fed sensorless speed control induction motor drives using model reference adaptive system," *Elect. Power Compon. Syst.*, vol. 42, no. 7, pp. 727–736, 2014.



- [8] D. Zhou, J. Zhao, and Y. Liu, "Predictive torque control scheme for three-phase four-switch inverter-fed induction motor drives with DC-link voltages offset suppression," *IEEE Trans. Power Electron.*, vol. 30, no. 6, pp. 3309–3318, 2015.
- [9] Hany M. Hasanien and S. M. Mueeen, "Particle swarm optimization-based superconducting magnetic energy storage for low-voltage ride-through capability enhancement in wind energy conversion system," *Elect. Power Compon. Syst.*, vol. 43, no. 11, pp. 1278–1288, 2015.
- [10] Hany M. Hasanien, "Shuffled frog leaping algorithm-based static synchronous compensator for transient stability improvement of a grid-connected wind farm," *IET Renew. Power Gener.*, vol. 8, no. 6, pp. 722–730, 2014.
- [11] M. N. Ambia, H. M. Hasanien, A. Al-Durra, and S. M. Mueeen, "Harmony search algorithm-based controller parameters optimization for a distributed-generation system," *IEEE Trans. Power Del.*, vol. 30, no. 1, pp. 246–255, Feb. 2015.
- [12] Hany M. Hasanien, "Design optimization of PID controller in automatic voltage regulator system using Taguchi combined genetic algorithm method," *IEEE Syst. J.*, vol. 7, no. 4, pp. 825–831, 2013.
- [13] Hany M. Hasanien, "Performance improvement of photovoltaic power systems using an optimal control strategy based on whale optimization algorithm," *Electric Power Syst. Research.*, vol. 157, pp. 168–176, 2018.
- [14] Hany M. Hasanien, "Gravitational search algorithm-based optimal control of archimedes wave swing-based wave energy conversion system supplying a DC microgrid under uncertain dynamics," *IET Renew. Power Gener.*, vol. 11, no. 6, pp. 763–770, 2017.
- [15] Hany M. Hasanien and M. Matar, "Water cycle algorithm-based optimal control strategy for efficient operation of an autonomous microgrid", *IET Gener. Transm. Distrib.*, vol. 12, no. 21, pp. 5739–5746, 2018.
- [16] S. Mirjalili, S. M. Mirjalili, and A. Lewis, "Grey wolf optimizer," *Adv. Eng. Soft.*, vol. 69, no. 3, pp. 46–61, 2014.
- [17] C. Muro, R. Escobedo, L. Spector, and R. Coppinger, "Wolf-pack (*Canis lupus*) hunting strategies emerge from simple rules in computational simulations," *Behav. Process.*, vol. 88, no. 3, pp. 192–197, 2011.
- [18] Attia A. El-Fergany and Hany M. Hasanien, "Single and multi-objective optimal power flow using grey wolf optimizer and differential evolution algorithms," *Elect. Power Compon. Syst.*, vol. 43, no. 13, pp. 1548–1559, 2015.
- [19] C. Olalla, R. Leyva, A. El Aroudi, and I. Queinnec, "Robust LQR control for



PWM converters: an LMI approach,” IEEE Trans. Ind. Electron., vol. 56, no.7, pp. 2548–2558, 2009.

[20] K. Ogata, “Modern control engineering,” PHI Learning Private Limited, 2011.

[21] M. J. Mahmoodabadi and N. R. Babak, “Robust fuzzy linear quadratic regulator control optimized by multi-objective high exploration particle swarm optimization for a 4 degree-of-freedom quadrotor,”

Aerospace Sc. Tech., vol. 97, 105598, pp. 1–13, Feb. 2020.

[22] H. Zhang, J. Umenberger and X. Hu, “Inverse optimal control for discrete-time finite-horizon linear quadratic regulators,” Automatica, vol. 110, 108593, pp. 1–9, December 2019.

[23] C. Possieri, M. Sassano, S. Galeani, and A. R. Teel, “The linear quadratic regulator for periodic hybrid systems,” Automatica, vol. 113, 108772, pp. 1–12, March 2020.